Experimental study on the radiant heat flux of wall-attached fire plume generated by rectangular sources

Xianjia Huang[a], Yuhong Wang[b], He Zhu[b], Le He[b], Fei Tang[*, c], Jennifer Wen[*, d]

[a] Joint Laboratory of Nuclear Power Plant Fire Safety, Institute of Industry Technology, Guangzhou & Chinese Academy of Sciences, Guangzhou 511458, China
[b] State Key Laboratory of Nuclear Power Monitoring Technology and Equipment China Nuclear Power Design Co., Ltd., Shenzhen 518045, China
[c] School of Automotive and Transportation Engineering, Hefei University of Technology, Hefei, Anhui 230009, China
[d] School of Engineering, University of Warwick, Coventry CV4 7AL, UK

*Corresponding author:
Email address: ftang@hfut.edu.cn; jennifer.wen@warwick.ac.uk
Postal address: School of Automotive and Transportation Engineering, Hefei University of Technology, Hefei, Anhui, 230009, China

Abstract

Radiant heat flux of fire plume is an essential parameter indicating the hazards of a fire. In this work, fire experiments of a wall-attached fire with different aspect ratios were conducted. In addition, the effect of the sidewall on mean flame height and radiant heat flux of the rectangular fire was investigated. The sidewall causes a decrease in air entrainment; therefore, the mean flame height is observed to increase. The radiant heat flux increased owing to the increase in flame height and thermal radiation from the heated sidewall. Experimental results of the mean flame height are consistent with those predicted by an existing model. This validated the reliability of the experimental setup for a rectangular wall-attached fire. Furthermore, a model based on the increase in flame height and thermal radiation from the heated sidewall was developed to estimate the radiant heat flux from a rectangular wall-attached fire. The error in prediction was less than 15% for this model.

Key words: Rectangular fire source; Sidewall; Wall-attached fire; Mean flame height; Radiant heat flux

Nomenclature

c_p	Specific heat of ambient air, kJ/kg·K
c_s	Specific heat of sidewall, kJ/kg·K
D	Equivalent diameter, m
$\overline{D}$	Hydraulic diameter, m
F	Geometry view factor
g	Acceleration due to gravity, m/s^2
L	Length of rectangular fire source, m
L_f	Mean flame height, m
L_t	Path length, m
m_s	Mass of sidewall, kg
n	Percentage
W	Width of rectangular fire source, m
P^*	Effective perimeter, m
pi	Circular constant
$\dot{q}''$	Radiant heat flux, kW/m^2
$\dot{Q}$	Heat release rate, kW
$\dot{Q}^*$	Dimensionless heat release rate
$\dot{Q}^*_{wp}$	Dimensionless heat release rate based on effective perimeter
R_0	Distance between the target and the virtual point, m
R_H	Fractional relative humidity
S	Saturated water vapor pressure at the atmospheric temperature, mmHg
T	Temperature, K
T_0	Initial temperature, K
T_∞	Ambient temperature, K
V_s	Volume of sidewall, m^3

Greek symbols

Γ	Transmissivity of atmosphere
γ	Atmosphere transmissivity to thermal radiation
θ	Angel between the connecting line and the target surface normal
ε	Flame emissivity
ρ_s	Density of sidewall, kg/m^3
ρ_∞	Ambient density, kg/m^3
σ	Stefan–Boltzmann constant, 5.67×10^{-8} $W/(m^2K^4)$
τ	Transmissivity
τ_a	Transmissivity of thermal radiation in the air
τ_s	Transmissivity of thermal radiation in the smoke
χ_r	Radiative fraction

1. Introduction

The shape of the fire source has a considerable effect on flame characteristics [1]. Rectangular fire sources are common and have recently attracted widespread attention from the research community [1-17]. The flame height, centerline temperature, and radiant heat flux of a flame generated by a rectangular fire source have been widely investigated [1-7]. Furthermore, the effect of atmospheric pressure on the burning behavior of a rectangular fire source was studied numerically [8-13]. Recently, Ji et al. [14] and Liu et al. [15] investigated the influence of sidewalls on the burning behavior of a rectangular fire source. Liu et al. [16] and He et al. [17] studied the interaction of two rectangular fires.

The behavior of fire is considerably influenced by a sidewall. Zukoski et al. [18] found that the air entrainment of a fire source located against a sidewall was reduced to 43% as compared to the fire in an open space. Hasemi and Tokunaga [19] measured the height of flame tips and continuous flames generated by a fire source located against a sidewall. The existence of walls near a fire source was anticipated to suppress the growth of the eddy scale in the plume. Poreh and Garrad [20] investigated the flame height and mass flux of a pool fire close to a wall. These models overestimated the mean flame height by approximately 15–30%. Tang et al. [21] studied the effect of cross-wind on near-wall buoyant turbulent diffusion flame length and tilt. Ji et al. [22, 23] studied the influence of a sidewall on a pool fire in a corridor-like structure. The mass loss rate of pool fire was increased due to the heat sidewall. Hu et al. [24-26] investigated the fire behavior of gas jet fires and line-source gas fires constrained by two parallel sidewalls. Tao et al. [27-29] investigated the flame characteristics of buoyancy-controlled gas fire bounded by a sidewall and ceiling. Generally, the effect

of sidewalls on fire behavior is a blocking effect that prevents air entrainment. The flame height of gas fire is increased due to the decrease in air entrainment. However, a few characteristics of a fire source influenced by a sidewall require further study.

The radiant heat from a flame is one of the most important parameters indicating the hazards of a fire in open space. There have been some valuable studies focusing on pool fire [30-33]. Furthermore, some important studies have been conducted to predict the heat flux from a rectangular fire source. Tu et al. [9] and Tang et al. [12] measured the radiant heat flux in the far field of a rectangular fire source with aspect ratios ranging from 1 to 8. Fleury [34] conducted fire experiments using aspect ratios from 1 to 3. Six models, including a point source model, three cylindrical models, a basic correlation model, and a planar model, were used to estimate the radiant heat flux from a fire source. As an unexpected result, the point source model exhibited the best performance on average. Wan et al. [35] developed a cuboid flame model to predict the heat flux of two identical rectangular fire sources with an aspect ratio of 2 and a distance of 0 mm. The research above focus on the rectangular fire source in an open space. The influence of a sidewall on the radiant heat flux of buoyancy-controlled diffusion plumes generated by rectangular fires has not been investigated experimentally yet.

This study focuses on the effect of sidewalls on the radiant heat flux from a rectangular wall-attached fire with different aspect ratios. Fire experiments with rectangular burners of the same surface area but different aspect ratios were conducted against a calcium silicate board. For comparison, similar fire experiments are conducted with a rectangular fire source without a sidewall. The influence of a sidewall and its aspect ratios on the mean flame height and radiant heat flux discussed in this study. Furthermore, the model for the radiant heat flux of a rectangular fire against a sidewall is investigated.

2. Experimental method

2.1 Experimental setup

The schematic of the experimental setup is shown in Fig. 1 and propane were used as the fuel. The fire experiments were performed using one square and three rectangular burners. All the burners had the same surface area but different aspect ratios. The thermal properties and dimensions of calcium silicate board used for the sidewall are listed in Table 1.

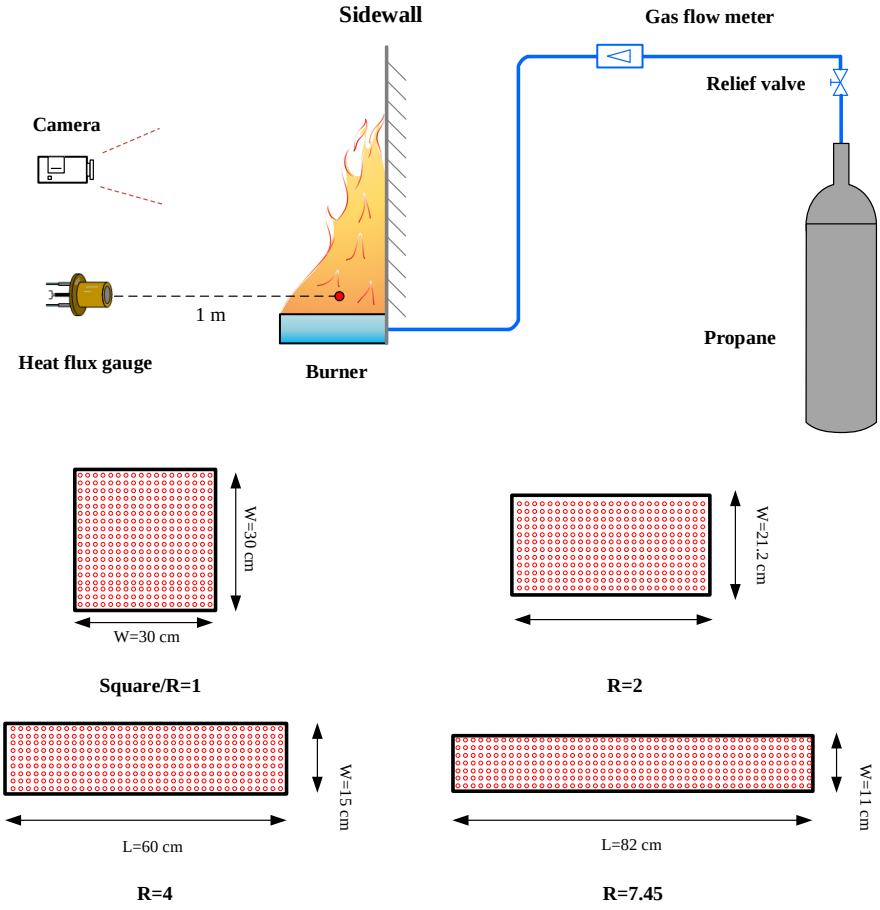

Fig. 1 Schematic of experimental setup

The selected burning surface area of 900 cm^2 was the same as in the literature [6, 7, 9]. The pool scale effect on the burning rate of a hydrocarbon pool fire is divided into three different regimes [8]: conduction-controlled, convection-controlled, and

radiation-controlled. When the equivalent diameter of the pool is longer than 0.2 m, the burning rate is dominated by the radiation directly from the flame. Therefore, the surface area of the burner was selected for studying the flame characteristics of a large pool fire. The details of the fire scenarios are listed in Table 2, and each fire test was repeated two times.

Table 1 Thermal properties of the fire-proof board

Materials	**Density (kg/m^3)**	**Conductivity (W/mK)**	**Sp. ht. cap. (kJ/kgK)**	**Length (m)**	**Width (m)**	**Thickness (m)**
calcium silicate	925	0.15	1.0	2.44	1.22	0.008

Table 2 Summary of fire scenarios

Burner shape	**Surface area (cm^2)**	**Burner**		**Aspect ratio R**	**Heat release rate $\dot{Q}$ (kW)**
		Length (cm)	**Width (cm)**		
Square	900	30.0	30.0	1	28.3; 42.4; 56.5; 70.7; 84.8
Rectangular	900	42.4	21.2	2	
Rectangular	900	60.0	15.0	4	
Rectangular	900	82.0	11.0	7.4	

The flame shape was recorded using a digital Charge Coupled Device (CCD) camera (resolution: 2592×1944 pixels) with a film of 25 frames/s. The binary image processing technology captures the flame shape and converts it into binary images. It first calculates the height of the flame in the binary image, and then converts it to the real height, as shown in Fig. 6. The mean flame height has been defined as the height at which the intermittency is 0.5 [6]. An STT-25-10R/WF type water-cooled heat flux gauge with a range up to 10 kW/m^2 and a measurement uncertainty $\pm$3% was placed with its radiation-receiving surface vertically. The temperature distribution on the back surface of the sidewall was recorded by an infrared camera (FLIR E85), as shown in

Fig. 2. The distance between the gauge and center of the burner was 1 m. The height of the gauge was in level with the burner surface.

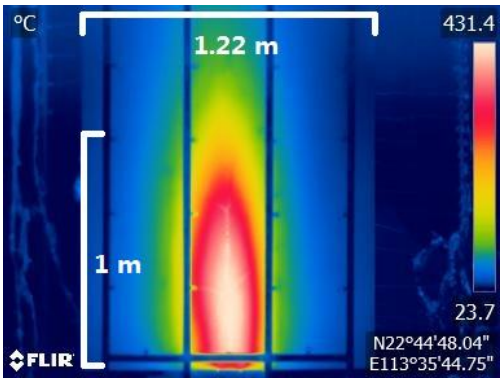

Fig. 2 Temperature distribution on the back of the sidewall (R = 1, $\dot{Q}$ = 84.8 kW)

2.2 Calibration of the fire experiment setup

Fire experiments were performed using axis-symmetric sources (square burners) used to calibrate the experimental setup. Fig. 3 shows a comparison among the mean flame heights generated by a square burner determined by the Heskestad model [36]. The experimental results conformed to those predicted by the Heskestad model [36].

$$L_f = \left(3.7Q^{*2/5} - 1.02\right)D \quad (1)$$

For a square burner, the equivalent diameter (D) is calculated using $2*\sqrt{s/pi}$, where *s* is the area of the square, which is equal to 0.34 m for the square burner in the present study. Q^* is dimensionless heat release rate of fire source and expressed as $\dot{Q}/\rho_\infty c_p T_\infty g^{1/2} D^{5/2}$.

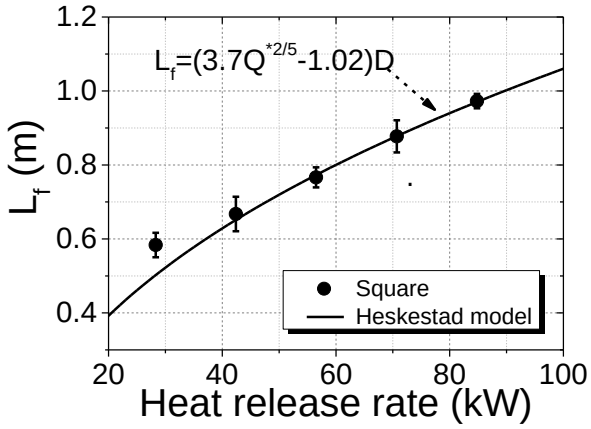

Fig. 3 Comparison among mean flame heights generated by square burners with those determined using the Heskestad model

Figure 4 compares the heat flux estimated by the cuboid flame and point source models with the experimental results for an axis-symmetric fire source [7]. The point source model assumes that all radiation comes from a single point at the center of the flame, and can be expressed as [7, 33]

$$\dot{q}'' = \gamma \frac{\chi_r \dot{Q}}{4\pi R_0^2} \cos\theta \tag{2}$$

For the cuboid flame model, the thermal radiation can be predicted as [7, 35]

$$\dot{q}'' = \gamma \frac{F\chi_r \dot{Q}}{4DL_f + D^2} \tag{3}$$

The cuboid flame and point source models exhibit good agreement with the experimental results [7]. The prediction by the cuboid flame model is a little better than the point source model. The prediction error is less than 10% for both models. This validated the reliability of the experimental results considering the radiant heat flux obtained using the proposed setup.

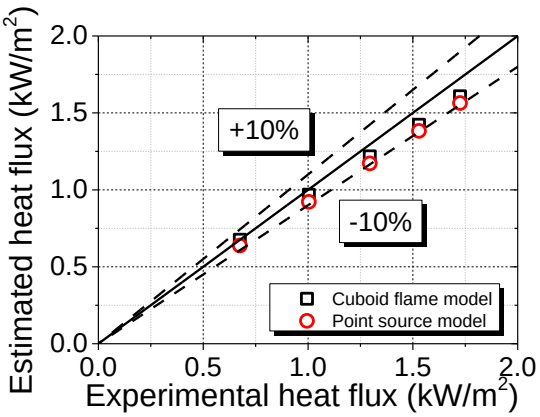

Fig. 4 Comparison between estimated heat flux by the cuboid flame and point source models with the experimental results for an axis-symmetric fire source [7]

3. Results and discussion

3.1 Flame morphology

Figure 5 shows the front view of the flame morphology for a rectangular fire source against a calcium silicate board. Figure 6 plots the contour image of flame height frequency for the rectangular fire source with different aspect ratios against the sidewall. The flame was divided into several sub-flames as the aspect ratio was increased to 7.45. A possible reason is that different air entrainment rates at different directions affect the burning process to give different flame shapes [6]. Compared with the rectangular fire source without a sidewall, as shown in [6], the existence of the sidewall leads to a decrease in the number of sub-flames for rectangular fires. The sidewall blocks the air entrained from the length of the burner. The air entrainment rates were reduced significantly compared to the rectangular fire source in open space. Therefore, less air interrupted the rectangular flame into the sub-flame.

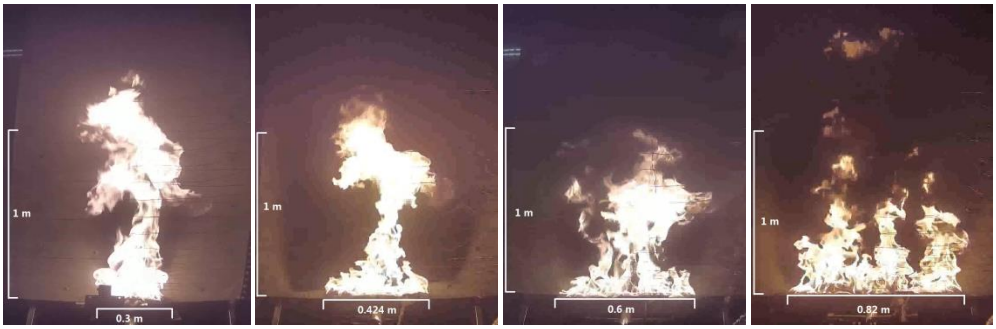

(a) Square (R = 1) (b) R = 2 (c) R = 4 (d) R = 7.45

Fig. 5 Flame morphology of rectangular fire source located against the sidewall ($\dot{Q}$ = 84.8 kW)

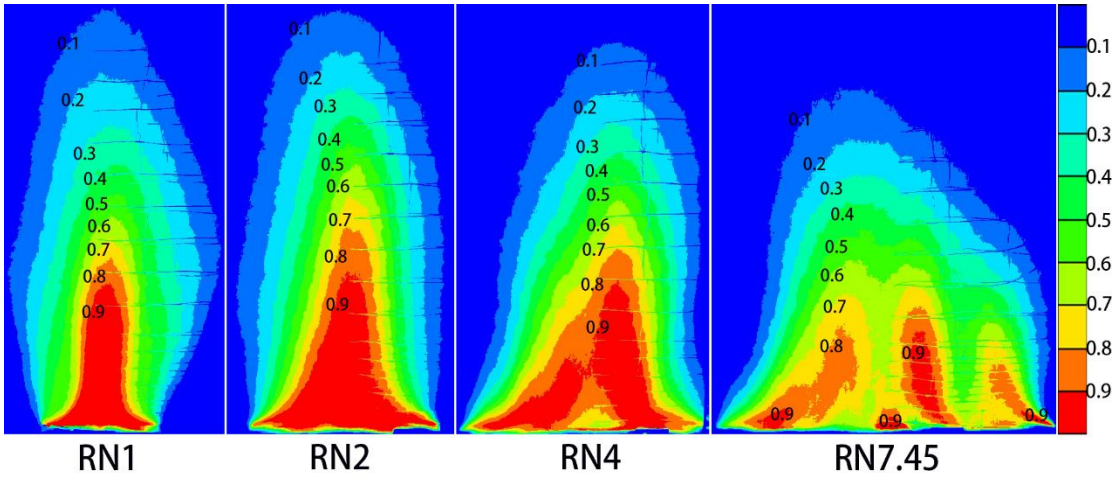

(a) Square (R = 1) (b) R = 2 (c) R = 4 (d) R = 7.45

Fig. 6 Contour image of flame height frequency for the rectangular fire source with different aspect ratios against the sidewall.

3.2 Mean flame height

The perimeter has an important effect on the air entrainment and mean flame height [20]. For free flames of a rectangular source of size L and W, the flame height was normalized by the perimeter 2(L + W) which was used as the length scale [26]. But for the rectangular fire source located against a sidewall, the mirror image (Eq. (4)) to plot the data as it was usually done [26, 37]. For a comparison, the appropriate effective

perimeter was 2(L + 2 W) was found to be an appropriate length scale, as described in [26] as:

$$P^* = 2(L + 2W), \qquad \text{With a sidewall} \tag{4}$$

Then, based on the fitness of the experimental data, the correlation between the mean flame height and dimensionless heat release rate was developed as described in [26]:

$$\frac{L_f}{P^*} = 5.47\dot{Q}_{wp}^{*\,2/3}, \quad \dot{Q}_{wp}^* \leq 0.3, \tag{5}$$

where $\dot{Q}_{wp}^*$ is dimensionless heat release rate of fire source against a sidewall and expressed as $2\dot{Q}/(\rho_\infty c_p T_\infty g^{\frac{1}{2}}(P^*)^{\frac{5}{2}})$.

Figure 7 shows the mean flame height of the rectangular wall-attached fire. The effective perimeter of the burner exhibited an inverse relationship with mean flame height. When the heat release rate was fixed, the mean flame height of the rectangular fire increased as the aspect ratio increased from 1 to 2 and decreased from 2 to 7.45. When the aspect ratio increased from 1 to 2, the effective perimeter of the rectangular fire source decreased from 1.8 m to 1.696 m, and the entrainment rate of air decreased. Therefore, the mean flame height increased as the aspect ratio increased. When the aspect ratio increased from 2 to 7.45, the effective perimeter of the rectangular fire source increased from 1.696 m to 2.12 m, which increased the air entrainment rate. Thus, the mean flame height decreased as the equivalent perimeter increased.

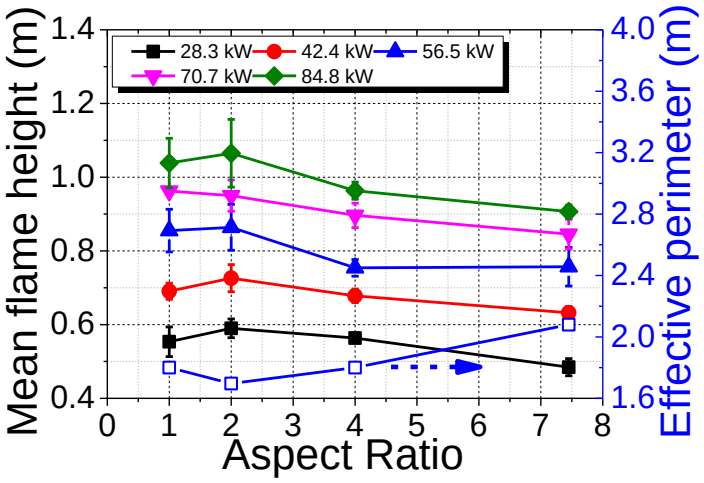

Fig. 7 Mean flame height of rectangular wall-attached fire

Figure 8 compares the obtained experimental data with the prediction made using Eq. (5). Generally, the experimental data for a fire source located against a sidewall is well estimated using Eq. (5), which was developed by Zhang et al. [26]. The experimental data obtained in the present study complement the validation of Eq. (5). This can be used for a fire source with a small dimensionless heat release rate ($0.01 < \dot{Q}^{*}_{wp} < 0.05$). Furthermore, the reliability of the experimental setup was validated for a rectangular fire source with a sidewall.

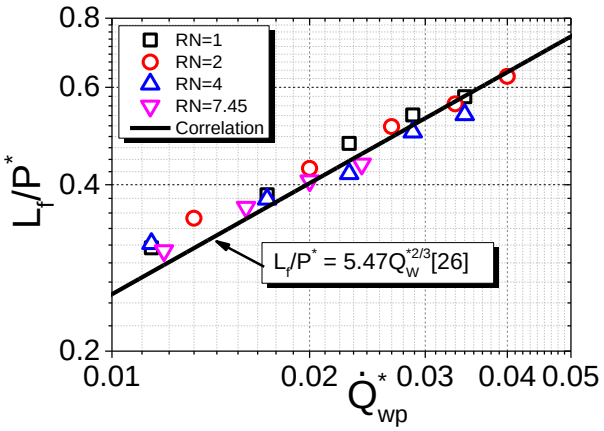

Fig. 8 Comparison of experimental data and the prediction made using Eq. (5)

3.3 Radiant heat flux

Figure 9 shows the radiant heat flux of rectangular fire with different boundary conditions. Compared with a rectangular fire source in an open space, introducing a sidewall increased the thermal radiation from the rectangular fire source. Two factors contributed to this increase: (1) the increase in flame height, as shown in Fig. 9 and [6], and (2) the thermal radiation from the heated calcium silicate sidewall plate.

Variation of the flame thickness have little effect on the thermal radiation from the rectangular wall-attached fire. The thickness of the rectangular wall-attached fire decreased from 0.3 m to 0.11 m as the aspect ratio of rectangular fire source changed from 1 to 7.45. According to Fig. 9(a), the maximum variation rate of thermal radiation is less than 10.5%, which is the ratio of the rectangular burner with R = 4 to that with R = 1 for the fire heat release rate at 76.7 kW.

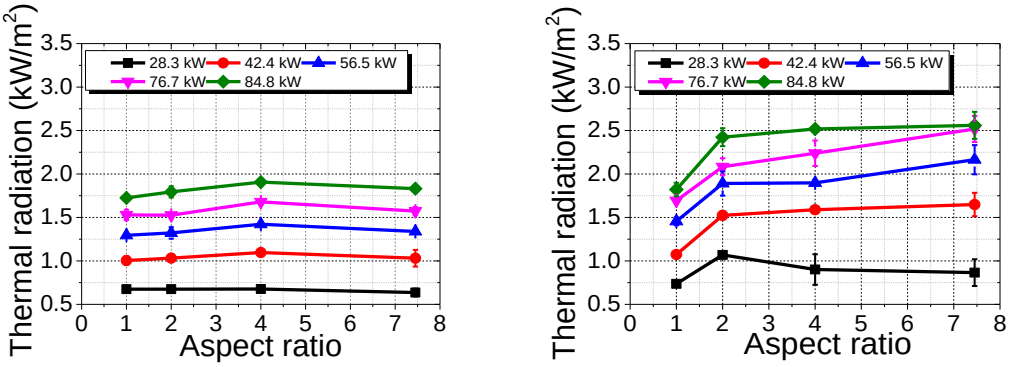

(a) open space [7] (b) with a sidewall

Fig. 9 Thermal radiation captured from the rectangular wall-attached fire with different boundary conditions

A conventional model was used for predicting the thermal radiation of rectangular fire sources in open space to estimate the radiant heat flux from the flame of a rectangular fire source with a sidewall [7, 33]. The model can be expressed as:

$$\dot{q}'' = \gamma \frac{F\chi_r \dot{Q}}{2WL_f + 2LL_f + WL} \quad . \tag{6}$$

To predict the thermal radiation from the heated calcium silicate sidewall plate, the sidewall was assumed to be an isothermally heated plate. The radiant heat flux from the heated sidewall can be calculated as:

$$\dot{q}'' = \tau F \varepsilon \sigma T^4 . \quad (7)$$

The convective heat loss from the heated sidewall to air was ignored.

The transmissivity of thermal radiation can be calculated as [38]:

$$\tau = \tau_a \cdot \tau_s . \quad (8)$$

The transmissivity of thermal radiation in the air (τ_a) can be estimated by [38, 39]:

$$\begin{aligned} \tau_a = {} & 1.006 - 0.0117\left(\log_{10} X(H_2O)\right) \\ & - 0.02368\left(\log_{10} X(H_2O)\right)^2 \\ & -0.03188\left(\log_{10} X(CO_2)\right) \\ & + 0.001164\left(\log_{10} X(CO_2)\right)^2 , \end{aligned} \quad (9)$$

where $X(H_2O)$ and $X(CO_2)$ are the amount of H_2O and CO_2 in the path, calculated by $X(H_2O) = 288.651 R_H L_t S/T_\infty$ and $X(CO_2) = L_t \cdot 273/T_\infty$, respectively.

The transmissivity of thermal radiation in the smoke was defined as follows [38, 40]:

$$\tau_s = e^{-0.02868D} . \quad (10)$$

Table 1 list the detailed value of thermal radiation for the heated sidewall. Generally, the transmissivity of thermal radiation was approximated to 0.93 as the aspect ratio varied from 1 to 7.45.

Table 1 Transmissivity of thermal radiation from the heated sidewall

Aspect ratio	τ_a	τ_s	τ
1	0.9369	0.9903	0.9279
2	0.9388	0.9903	0.9298
4	0.9402	0.9903	0.9311
7.45	0.9411	0.9903	0.9320

The temperature of sidewall was estimated as:

$$T - T_0 = \frac{n \cdot \dot{Q} \cdot t}{C_s m_s} . \tag{11}$$

The mass of the sidewall was calculated as:

$$m_s = \rho_s V_s . \tag{12}$$

Figure 10 compares the average temperature on the back of the sidewall and estimation by Eq. (11). The average temperature of the sidewall back was obtained based on the temperature distribution, as shown in Fig. 2. In comparison with the prediction, the experimental average temperature of the sidewall back is within the estimated temperature by the Eq. (11) with n = 5 % and n = 6 %. According to Zukoski et al. [18], the heat loss from the sidewall was estimated to be within 5% of the release rate for the square source fire. Therefore, the value of n was valued at 5% in the present work.

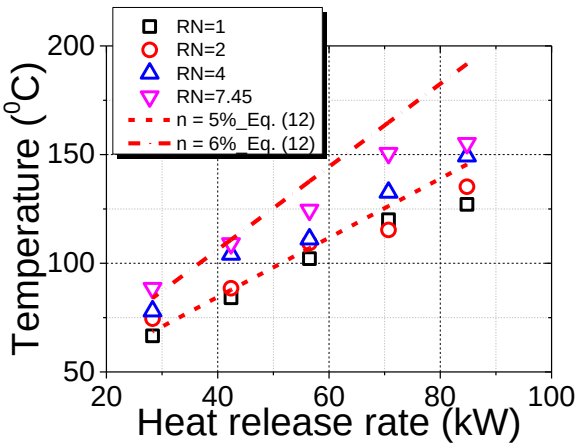

Fig. 10 Comparison between the average temperature of on the back of the sidewall and estimation by Eq. (11).

Figure 11 shows thermal radiation from the rectangular wall-attached fire and sidewall. The thermal radiation from the fire increased as the aspect ratio increased, while the effect of the variation of the aspect ratio on the thermal radiation from the sidewall was small. Figure 12 shows ratios of the thermal radiation from the sidewall to the rectangular wall-attached flame. For a certain heat release rate, the ratio decreased as the aspect ratio increased from 1 to 7.45. Generally, the ratio was within 13.6%–21.2%.

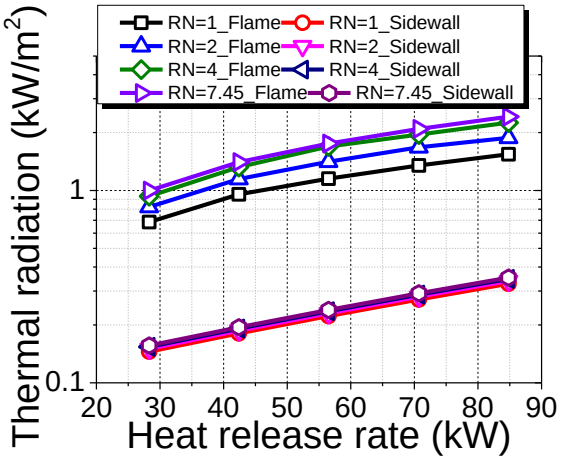

Fig. 11 Thermal radiation from the rectangular wall-attached fire and sidewall

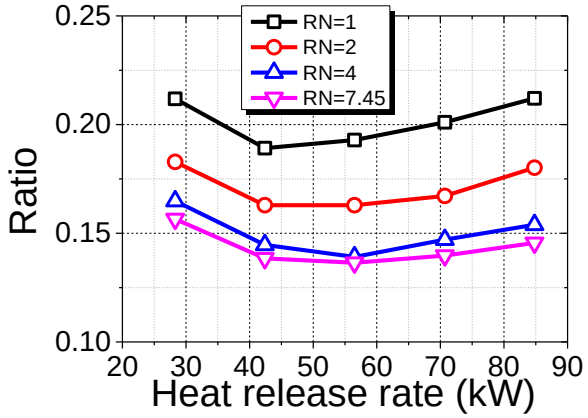

Fig. 12 Ratios of thermal radiation from the rectangular wall-attached fire to the sidewall

The duration of the fire was selected as 10 min. Based on Eqs. (6)–(12), the thermal radiation flux from a rectangular fire source with a sidewall can be calculated. The comparison of the estimated heat flux with the experimental data is shown in Fig. 13. The error of model prediction was less than 15%.

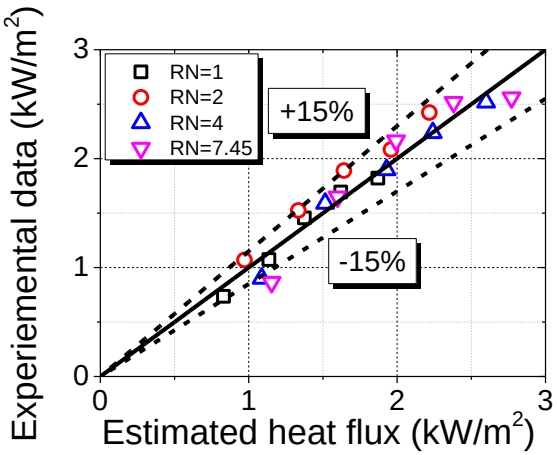

Fig. 13 Comparison of estimated heat flux with experimental data

4. Conclusions

This study focused on the flame behavior of a rectangular wall-attached fire source with different aspect ratios. Experiments with a rectangular fire source were conducted with different aspect ratios against a sidewall. The mean flame height and radiant heat flux of the rectangular fire with a sidewall were investigated. Notable findings of this study are as follows:

The mean flame height increased for a rectangular wall-attached fire due to a decrease in air entrainment. The mean flame height decreased as the aspect ratio increased, determining the effective perimeter of the rectangular fire source with a sidewall, as given by Eq. (4). The effective perimeter of the burner exhibited an inverse relationship with the mean flame height. Experimental results with the mean flame height in this study conform to the prediction by the model proposed by Zhang et al. [26]. This validated the reliability of our experimental setup for a rectangular fire source with the sidewall.

The radiant heat flux of the rectangular fire was higher for the fire source located against a sidewall. The increase in the mean flame height and thermal radiation from a heated sidewall led to an increase in radiant heat flux. The thermal radiation ratios from the sidewall to the rectangular wall-attached flame were within 13.6%–21.2%. Accounting for these two factors, the model for radiant heat flux was developed. Compared with experimental data, the error of the prediction model was less than 15%.

Acknowledgements

This work was supported jointly by the National Key Research and Development Program of China (Project No. 2016YFC0800100); Guangzhou Science and

Technology Plan Program of China (Project No. 202002030124), and National Nature Science Funds of China under Grant (No. 51776060).

References

[1] Hasemi Y, Nishihata M. Fuel shape effect on the deterministic properties of turbulent diffusion flames, Fire Saf. Sci 1987; 7:227-234.

[2] Qunitiere JG, Grove BS. A unified analysis for fire plumes, 27th Symposium on Combustion Institute. 1988. P. 2757-2766.

[3] Hu LH, Zhang XC, Zhang XL, et al. A re-examination of entrainment constant and an explicit model for flame heights of rectangular jet fires, Combust. Flame 2014; 161:3000-3002.

[4] Gao W, Liu NA, Jiao Y, et al. Flame length of buoyant turbulent slot flame, Proc. Combust. Inst. 2019; 3:3851-3858.

[5] Tang F. Cao ZL, Palacios A, Wang Q, A study on the maximum temperature of ceiling jet induced by rectangular-source fires in a tunnel using ceiling smoke extraction, Int. J. Therm. Sci., 2018; 127: 329-334 .

[6] Huang XJ, Zhuo XJ, Huang T, et al. Simple flame height correlation for buoyancy-controlled diffusion plumes generated by rectangular sources fire with different aspect ratios, Fuel 2019, 254: 115655.

[7] Huang XJ, Zhuo XJ, Huang T, et al. Thermal radiation model for the buoyancy-controlled diffusion plumes from rectangular fire sources, Int. J. Therm. Sci. 2020; 150: 106234.

[8] Hu LH, Tang F, Wang Q, et al. Burning characteristics of conduction-controlled rectangular hydrocarbon pool fires in a reduced pressure atmosphere at high altitude in Tibet, Fuel 2013;111:298-304.

[9] Tu R, Fang J, Zhang YM, et al. Effects of low air pressure on radiation-controlled rectangular ethanol and n-heptane pool fires, Proc. Combust. Inst. 2013; 34:2591-2598.

[10] Tang F, Hu LH, Qiu ZW, et al. A global model of plume axial temperature profile transition from axisymmetric to line-source pool fires in normal and reduced pressures, Fuel 2014;130:211-214.

[11] Zhang XC, Hu LH, Zhu W, et al. Axial temperature profile in buoyant plume of rectangular source fuel jet fire in normal- and a sub-atmospheric pressure, Fuel 2014;134:455-459.

[12] Tang F, Zhu KJ, Dong MS et al. Mean flame height and radiative heat flux characteristic of medium scale rectangular thermal buoyancy source with different aspect ratios in a sub-atmospheric pressure, Int. J. Heat Mass. Transf. 2015; 84:427-432.

[13] Hu LH, Zhang XC, Zhang XL, et al. Flame heights and fraction of stoichiometric air entrained for rectangular turbulent jet fires in a sub-atmospheric pressure, Proc. Combust. Inst. 2017; 36:2995-3002.

[14] Ji J, Tan TT, Gao ZH, et al. Influence of sidewall and aspect ratio on burning behavior of rectangular ethanol and heptane pool fires, Fuel, 2019;238:166-172.

[15] Liu Q, Tao CF, Wang Peng, et al. The flame height of rectangular pool fires bounded by a sidewall with different distances and aspect ratios, J. Therm. Anal. Calorim. 2019, https://doi.org/10.1007/s10973-019-08093-z.

[16] Liu NA, Zhang SJ, Luo XS, et al. Interaction of two parallel rectangular fires, Proc. Combust. Inst. 2019; 37:3833-3841.

[17] He PX, Wang Peng, Wang Kai, et al. The evolution of flame height and air flow for double rectangular pool fires, Fuel 2019; 237:486-493.

[18] Zukoski EE, Kubota T, Cetegen B et al. Entrainment in Fire Plumes, Fire Saf. J. 1980/81; 3:107-121.

[19] Hasemi Y, Tokunaga T. Some Experimental Aspects of turbulent diffusion flames and buoyant plumes from fire sources against a wall and in a corner of walls, Combust Sci Technol, 1984; 40:1-17.

[20] Poreh M, Garrad G. A study of wall and corner fire plumes, Fire Saf. J. 2000; 34:81-98.

[21] Tang F, Li LJ, Wang Q, Shi Q, Effect of cross-wind on near-wall buoyant turbulent diffusion flame length and tilt, Fuel, 2016; 186: 350–357.

[22] Ji J, Fan CG, Li YZ, et al. Experimental study of non-monotonous sidewall effect on flame characteristics and burning rate of n-heptane pool fires, Fuel 2015;145: 228-233.

[23] Ji J, Fu YY, Fan CG et al. An experimental investigation on thermal characteristics of sidewall fires in corridor-like structures with varying width, Int. J. Heat Mass. Transf. 2015; 84:562-570.

[24] Hu LH, Liu SX, Zhang XL. Flame heights of line-source buoyant turbulent non-premixed jets with air entrainment constraint by two parallel side walls, Fuel 2017; 200:583-589.

[25] Wang Q, Tang F, Zhou Z, et al. Flame height of axisymmetric gaseous fuel jets restricted by parallel sidewall: Experiments and theoretical analysis, App Energy 2017; 206:1519-1526.

[26] Zhang XL, Hu LH, Delichatsios MA, et al. Experimental study on flame morphologic characteristics of wall attached non-premixed buoyancy driven turbulent flames, Appl. Energy 2019; 254:113672.

[27] Tao CF, Shen Y, Zong RW. Experimental study on virtual origins of buoyancy-controlled jet flame with sidewalls, Appl. Therm. Eng. 2016; 106:1088-1093.

[28] Tao CF, Shen Y, Zong RW, Tang F. An experimental study of flame height and air entrainment of buoyance-controlled jet flames with sidewalls, Fuel 2016; 183:164-169.

[29] Tao CF, He YP, Zhuang Y, et al. The investigation of flame length of buoyancy-controlled gas fire bounded by wall and ceiling, Appl. Therm. Eng. 2017; 127:1172-1183.

[30] Sun B, Guo K, Pareek VK. Dynamic simulation of hazard analysis of radiations from LNG pool fire, J. Loss Prev. Proc., 2015; 35:200-210.

[31] Hu LH. A reviewer of physics and correlations of pool fire behavior in wind and future challenges, Fire Safety J, 2017; 91:41-55.

[32] Yi H, Feng Y, Wang QS. Computational fluid dynamics (CFD) study of heat radiation from large liquefied petroleum gas (LPG) pool fires, J. Loss Prev. Proc., 2019; 61:262-274.

[33] Zhou KB, Wang XZ. Thermal radiation modeling of pool fire with consideration on the non-uniform temperature in flame volume, Int. J. Therm. Sci. 2019; 138:12-23.

[34] Fleury R. Evaluation of thermal radiation models for fire spread between objects, Thesis, University of Canterbury, New Zealand, 2010.

[35] Wan HX, Gao ZH, Ji J, et al. Predicting heat fluxes received by horizontal targets from two buoyant turbulent diffusion flames of propane burning in still air, Combust. Flame, 2018; 190:260-269.

[36] Heskestad G. Fire Plumes, Flame height, and Air entrainment, SFPE handbook of fire protection engineering, 5th ed, 2016.

[37] Karlsson B, Quintiere JG, Enclosure fire dynamics, CRC Press LLC (2000)

[38] Shen GS, Zhou KB, Wu F, et al. A model considering the flame volume for prediction of thermal radiation from pool fire, Fire Tech. 2019; 55:129-148.

[39] Wayne FD, An economical formula for calculating atmospheric infrared transmissivities, J. Loss Pre. Ind. 1991; 4:86-92.

[40] Raj PK, Large hydrocarbon fuel pool fires: physical characteristics and thermal emission variations with height. J. Hazard. Mater. 2007; 140:280-292.